Journal of Magnetic Resonance **153,** 144–150 (2001)
doi:10.1006/jmre.2001.2428, available online at http://www.idealibrary.com on IDEAL®

COMMUNICATIONS

Hadamard Excitation Sculpting

Krish Krishnamurthy

Discovery Chemistry Research, Lilly Research Laboratories, Indianapolis, Indiana 46285

E-mail: krishk@lilly.com

Received May 9, 2001; revised August 10, 2001; published online October 5, 2001

An approach to Hadamard phase encoding and editing in an excitation sculpting experiment is presented. When band- and/or frequency-selective experiments are performed at more than one site using excitation sculpting, use of Hadamard excitation sculpting (HEX sculpting) will reduce the total measuring time to achieve a target S/N. The application of HEX sculpting is demonstrated using selective 1D and NOESY1D experiments.

Key Words: **excitation sculpting; Hadamard spectroscopy; NOESY1D; multiple-selective excitation; DPFGSE.**

INTRODUCTION

Excitation sculpting (*1*) is a powerful selective excitation experiment and probably the most efficient way to achieve selectivity in a NMR experiment, since it associates very clean frequency selection with "user-friendliness." Excitation sculpting is produced by the application of a double pulse field gradient spin-echo sequence (DPFGSE) as shown in Fig. 1A. Selective excitation using a DPFGSE train requires no additional phase cycling. The magnetization returns to its starting position at the end of the DPFGSE train, the excitation profile depending only on the inversion profile of the band-selective π pulses (S_1 and S_2). The phase of the magnetization is unaffected and the amplitude of the magnetization is scaled by the inversion profile of the π pulses and by loss due to relaxation during the spin echo. Single or multiple frequencies or bands can be simultaneously sculptured by employing appropriate "multiple-frequency"-shifted laminar pulses (SLP pulses) (*2*). In exciting a multiplet, the DPFGSE refocuses the evolution of scalar coupling. However, coupling *between* spins that are within the selected band(s) are not refocused. These advantages were quickly appreciated, and the DPFGSE method has recently enjoyed undeniable success in both frequency-selective 1D experiments such as NOESY1D and band-selected 2D experiments (*3–9*). While the 1D (or band-selective 2D) variations of two-dimensional experiments afford spectral simplification by focusing on the resonance(s) of interest, it is typically argued that two-dimensional spectroscopy affords much higher sensitivity since it benefits from the multiplex advantage, gathering information about all correlations simultaneously. Gathering information from N simultaneous measurements is more efficient in terms of sensitivity than performing N single experiments one after another (*9*). Freeman and coworkers (*10, 11*) recently pointed out that the strategy of simultaneous multisite excitation, where employing a coding scheme based on Hadamard matrices (*12*) can substantially reduce the total measuring time to achieve a target S/N. This principle was effectively used in the measurement of long-range proton–carbon coupling constants (*13, 14*). In this communication we describe the implementation of Hadamard encoding in DPFGSE experiments (*H*adamard *ex*citation sculpting—HEX sculpting) and demonstrate its application in NOESY1D experiments.

RESULTS AND DISCUSSION

In Fig. 2 the results of single- and multiple-frequency excitation sculpting (using the pulse sequence in Fig. 1A) are presented. In a typical application of excitation sculpting the two selective pulses (S_1 and S_2) are kept to be the same. However, as was pointed out by Shaka and co-workers in their article (*1*), this needs not be the case. In a two-site excitation sculpting one typically generates a "double-frequency" shifted laminar inversion pulse with the resultant shape being the linear combination of the "single-frequency" shifted pulses. If the nominal phase (*15*) of the two single-frequency shifted pulses is the same (say, x), then one generates a double-frequency shifted pulse (S_{xx}) that effects the RF event (inversion/refocusing) about the same axis (i.e., x axis) for both sites. If the nominal phase of the two single-frequency shifted pulses are quadrature shifted from one another (x and y), then one generates a double-frequency shifted pulse (S_{xy}) that effects the RF event about the x axis for one frequency and the y axis for the second frequency. The resultant effect of the S_{xx} and S_{xy} *inversion* pulses will be academic and for all practical purposes will generate the same inversion profile at both frequencies. However the effects of S_{xx} and S_{xy} *refocusing* pulses (as in a spin echo—or gradient spin echo) are clearly different. While spin echo using the S_{xx} pulse generates

1090-7807/01 $35.00

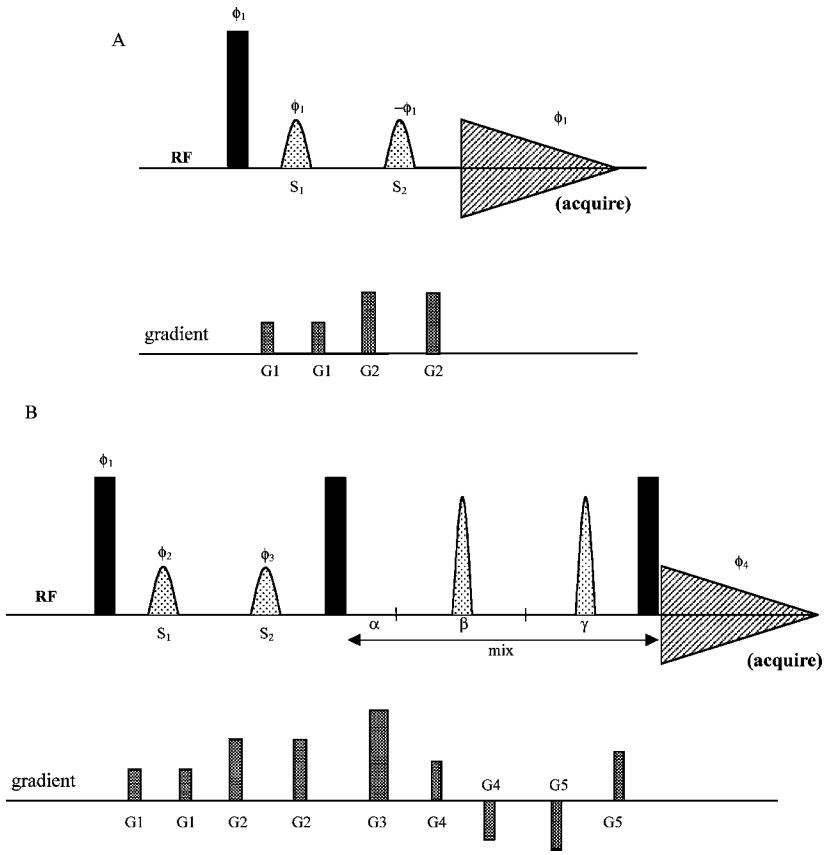

FIG. 1. Pulse sequences for (A) the double PFG spin echo and (B) HEX-NOESY1D. Vertical lines represent 90° pulses. The band-selective pulses are π pulses. The PFG echo times are set to minimum values to accommodate the gradient pulses, the band-selective pulses, and the gradient recovery delays. Sequence (A) does not include any basic phase cycling. The phase cycling used for sequence (B) is $\phi_2 = x, y, \phi_3 = x, x, y, y$ and $\phi_4 = x, -x, -x, x$. In addition a four-step Cyclops is introduced independently on ϕ_1, ϕ_2, and ϕ_3 with appropriate phase shift of the receiver. Phases not shown are along the x axis. The delays α, β, and γ are set in the ratio of 0.02 : 0.58 : 0.4.

in-phase echos for the two frequencies, the S_{xy} pulse will generate anti-phase echos for the two frequencies. Since the excitation sculpting train involves a "double" spin echo, use of either S_{xx} or S_{xy} in the place of *both* S_1 and S_2 will generate the same in-phase echoes for the two frequencies. However the excitation sculpting achieved with $S_1 = S_{xx}$ and $S_2 = S_{xy}$ (or $S_1 = S_{yy}$ and $S_1 = S_{xy}$) would have the two frequencies anti-phase with respect to each other (Figs. 3d, 3e). One can treat these two spectra ($S_1 = S_{xx}$, $S_2 = S_{xx}$ and $S_1 = S_{xx}$, $S_2 = S_{xy}$) as the component of a Hadamard H_2 matrix generating $1_{(+)}2_{(+)}$ and $1_{(+)}2_{(-)}$ spectra, where (+) and (−) represent the positive and negative phase, respectively, for the selected bands. Addition and subtraction of these two will now generate two subspectra that have *only* band 1 or band 2, respectively (Figs. 3f, 3g). The addition (or subtraction) of the two spectra in Figs. 3d and 3e increases the signal intensity by a factor of 2, while the noise is increased only by a square root of 2, thus resulting in S/N being increased by the square root of 2. For comparison, single-frequency selected 1D spectra acquired under identical experimental conditions using DPFGSE are presented in Figs. 3b and 3c. One can extend this principle to four bands and generate four spectra with the S_1 pulse being the same (S_{xxxx}) in all four cases, while the S_2 pulse is set to S_{xxxx}, S_{xxyy}, S_{xyxy}, and S_{xyyx}. The four spectra will have relative phases representative of a Hadamard H_4 matrix (Figs. 4e–4h) and can be "edited" by appropriate linear combination (Figs. 4j–4m). The spectra in Figs. 4j–4m were generated as follows: 4l = 4e + 4f + 4g + 4h; 4k = 4e + 4f − 4g − 4h; 4l = 4e − 4f + 4g − 4h; and 4m = 4e − 4f − 4g + 4h. Again, for comparison single-frequency selected DPFGSE spectra are presented in Figs. 4a − 4d. The four HEX sculptured spectra in Figs. 4e–4h were acquired over 8 scans each and the single-frequency excitation sculptured spectra in Figs. 4a–4d were also acquired over 8 scans, each under identical acquisition conditions. The S/N gain achievable using HEX sculpting followed by Hadamard editing compared to individual experiments done over the same total experiment time is clearly evident.

To explore the applicability of HEX sculpting in typical 1D experiments we investigated the HEX-sculptured NOESY1D pulse sequence (*7*) shown in Fig. 1B. The NOESY1D results

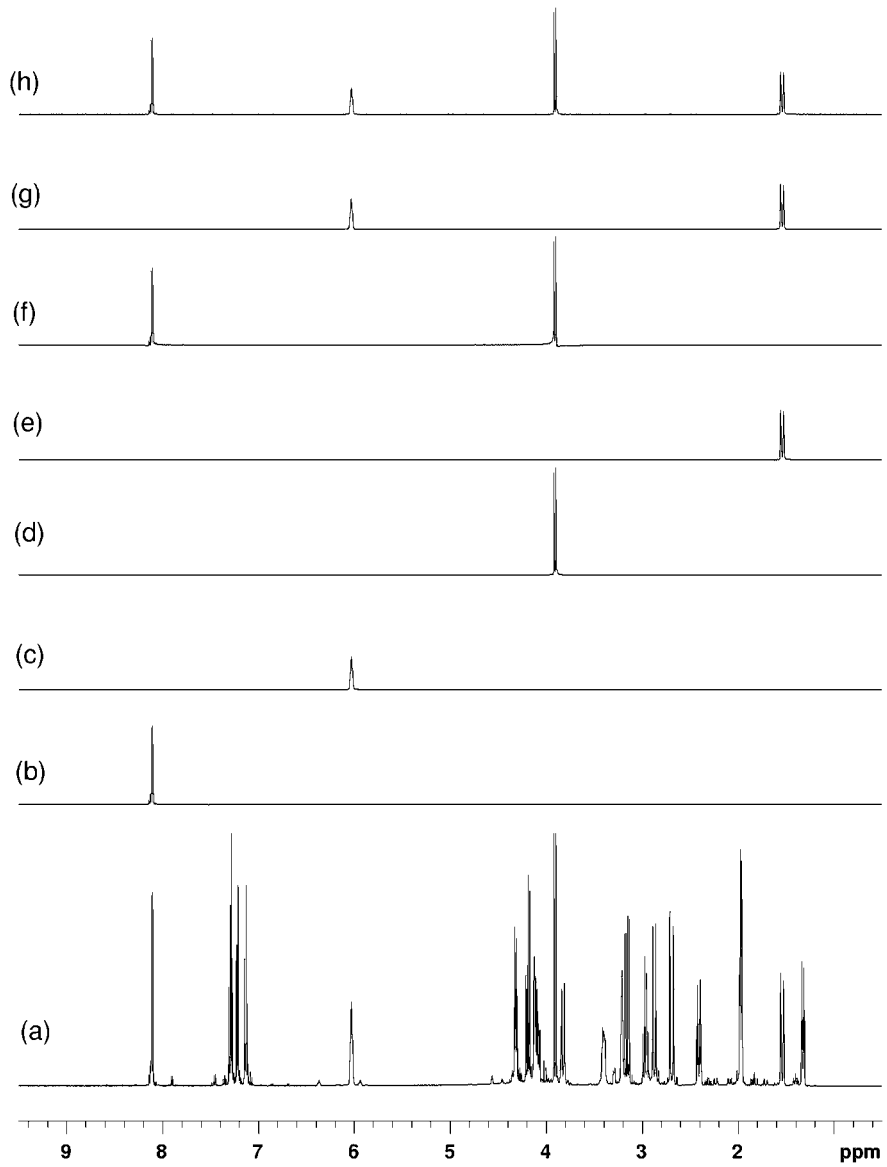

FIG. 2. Single- and multiple-frequency selected DPFGSE spectra of strychnine in CDCl3. (a) High-resolution reference spectrum, and (b–h) single- or multiple-frequency selected 1D spectra obtained using the pulse sequence in Fig. 1A. The band-selective π pulses ($S_1 = S_2$) are Q3 pulses with phase modulation to invert the selected resonance(s). All spectra were acquired with eight scans each.

using a sample of strychnine (10 mg/0.75 ml of CDCl3) are presented in Figs. 5 and 6. Four representative resonances (centered at 8.11, 6.05, 3.92, and 1.54 ppm with bandwidths of 55, 55, 45, and 50 Hz, respectively) were selected for this investigation. In Figs. 5a–5d are 1D NOESY spectra of the individual resonances. In each case both the S_1 and S_2 pulses are Q3 Gaussian cascade (*16*) applied as a single-frequency shifted laminar pulse with appropriate phase ramp to generate off-resonance inversion. A 500-ms nOe mixing time was used. Unedited HEXsculptured NOESY1D spectra for these four resonances are presented in Figs. 5e–5h. These were collected with the S_1 pulse set to S_{xxxx} and the S_2 pulse set to S_{xxxx} (Fig. 5e), S_{xxyy} (Fig. 5f), S_{xyxy} (Fig. 5g), or S_{xyyx} (Fig. 5h). The shape S_{xxxx} represents a quadruple-frequency shifted laminar Q3 Gaussian cascade pulse for generating simultaneous inversion at the four off-resonance frequencies with the nominal phase of all four being along the x axis. The other three shapes (S_{xxyy}, S_{xyxy}, and S_{xyyx}) are identical to the S_{xxxx} shape except for the nominal phase of the individual phase ramp. All four spectra (5e–5h) have nOe peaks from all four selected resonances except the phase of the nOe peaks from each resonance is differently coded. Appropriate linear combination of these will result in sorting out the individual sets. The spectra in Figs. 5j–5m were generated as follows: 5j = 5e + 5f + 5g + 5h; 5k = 5e + 5f − 5g − 5h; 5l = 5e − 5f + 5g − 5h;

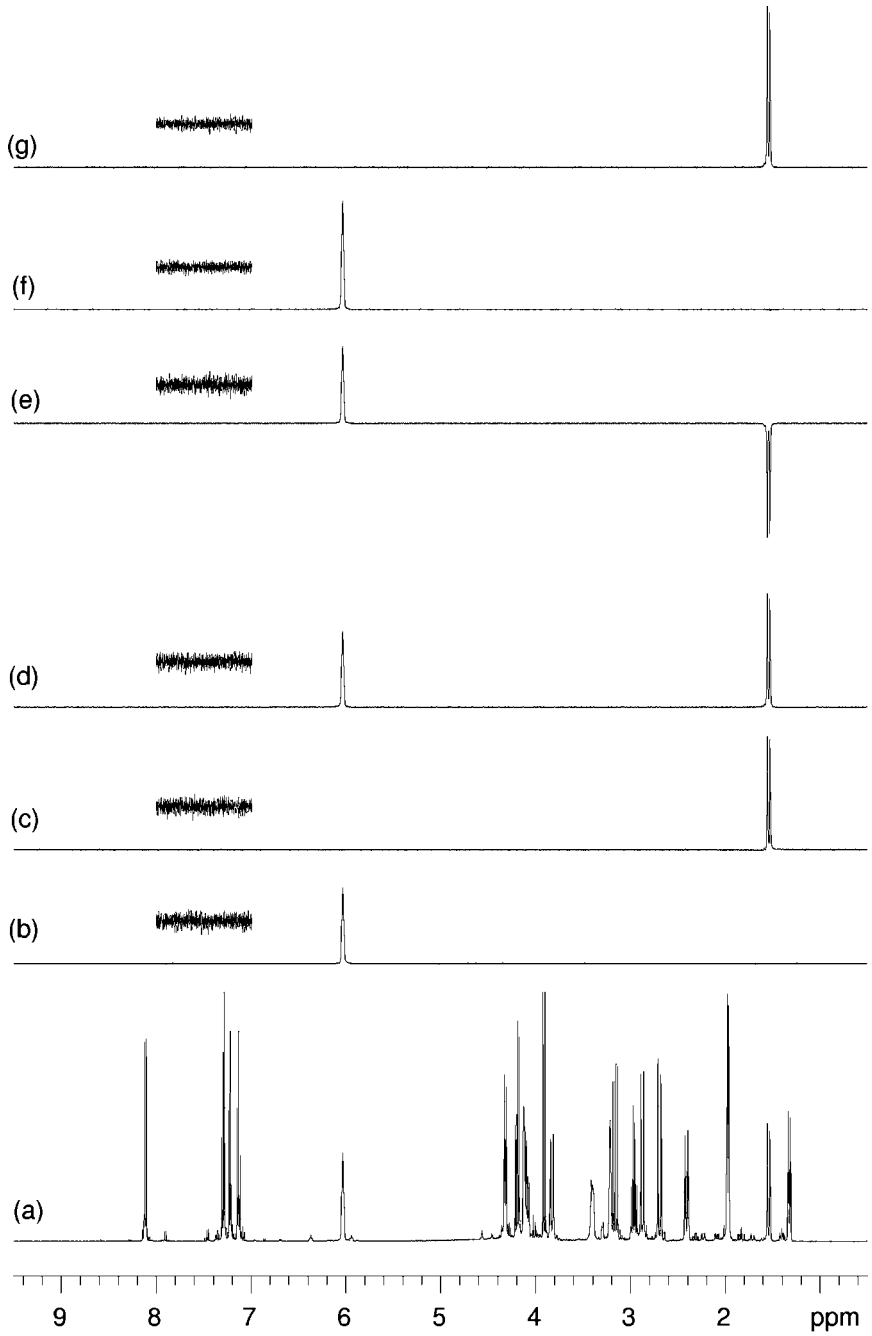

FIG. 3. Double-frequency selected HEX (*H*adamard *ex*citation) sculpted spectra of strychnine in CDCl3. (a) High-resolution reference spectrum, (b, c) single-frequency selected DPFGSE spectra with $S_1 = S_2$, (d) double-frequency selected HEX spectrum with $S_1 = S_2 = S_{xx}$, (e) double-frequency selected HEX spectrum with $S_1 = S_{xx}$ and $S_2 = S_{xy}$, (f) Hadamard-edited spectrum resulting from the sum of (d) and (e), and (g) Hadamard-edited spectrum resulting from the difference of (d) and (e). The selective 1D spectra were obtained using the pulse sequence in Fig. 1A. The band selective π pulses (S_1 and S_2) are single- or double-frequency shifted laminar Q3 pulses. S_{xx} and S_{xy} represent that the nominal phase of the two frequency-shifted waveforms are either in-phase (x and x) or quadrature shifted (x and y) with respect to each other, respectively. All selective excitation spectra were acquired with eight scans each. A 1.0-ppm noise region from each spectrum is further expanded.

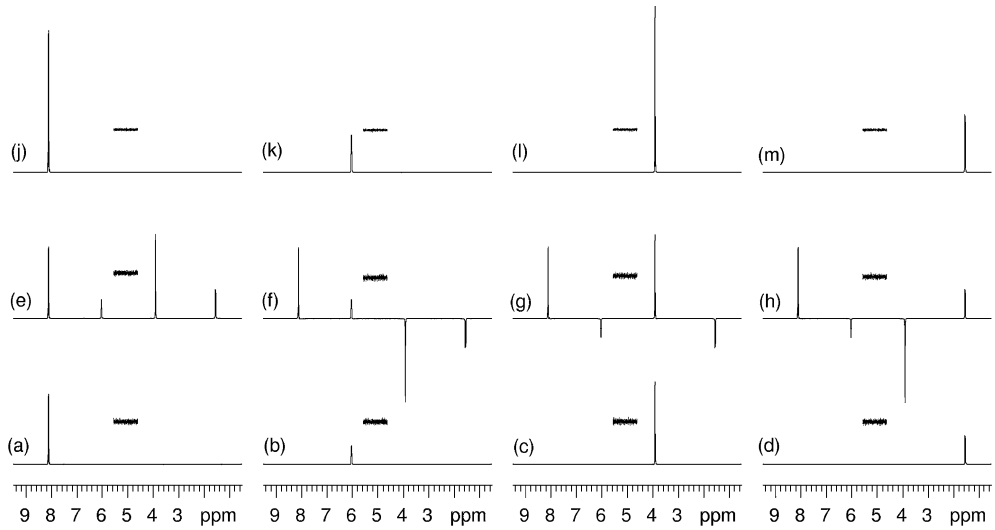

FIG. 4. Quadruple-frequency selected HEX-sculpted spectra of strychnine in CDCl3. (a–d) Single-frequency selected DPFGSE spectra with $S_1 = S_2$, (e–h) quadruple-frequency selected HEX spectra with $S_1 = S_{xxxx}$ and $S_2 = S_{xxxx}$, S_{xxyy}, S_{xyxy}, and S_{xyyx}, and (j–m) Hadamard-edited spectra resulting from an appropriate linear combination of the spectra in (e–h). The spectra were obtained using the pulse sequence in Fig. 1A. The band-selective π pulses (S_1 and S_2) are frequency-shifted laminar Q3 pulses. S_{xxxx}, S_{xxyy}, S_{xyxy}, and S_{xyyx} represent that the nominal phase of the quadruple-frequency shifted waveforms are either in-phase (x and x) or quadrature shifted (x and y) with respect to each other. All spectra were acquired with eight scans each. A 1.0-ppm noise region from each spectrum is further expanded.

and 5m = 5e − 5f − 5g + 5h. It should be noted that the total experiment time for the spectra in 5a–5d is same as that for the spectra in 5e–5h. As expected the "edited" spectra in 5j–5m shows an S/N improvement over the "individual" spectra in 5a–5d by a factor of 2 (square root of 4). In other words, to reach the same S/N as in the "edited" HEX-NOESY1D, the single-frequency selected NOESY1D experiments must be run four times longer. For comparison purposes, single-frequency selected NOESY1D spectra with the number of scans in each case increased by a factor of 4 were collected. In Fig. 6, these results (6j–6m) are compared to the HEX-edited NOESY1D experiments (6e–6h) . The S/N of the edited HEX-NOESY1D collected over a total experiment time of 18 min is comparable to that of the individual experiments collected over a total experiment time of over 1 h.

EXPERIMENTAL

All spectra were recorded at 25°C on a Varian Unity INOVA 500-MHz NMR spectrometer equipped with a Programmable Pulse Modulator in the proton channel and a gradient accessory and using a 1H{X} indirect detection probe. All nonselective rectangular pulses were of 9.7 μs duration. The nonselective broadband inversion pulses during the mixing time in the NOESY1D sequence are unshifted hyperbolic secant pulses of 1.5 ms duration. The band-selective π pulses (S_1 and S_2) in the DPFGSE train are Gaussian cascade Q3 pulses with appropriate phase modulation(s) to shift the center(s) of the inversion profile(s) to the required offset(s) as noted in the figure captions. All shaped pulses were generated using the Pandora's Box pulse shaping program (*17*) available in Varian NMR software. The gradients were rectangular shaped. Their amplitudes were set to G1 : G2 : G3 : G4 : G5 = 2 : 10 : 2 : 2 : 2 G/cm while the durations were set to G1 : G2 : G3 : G4 : G5 = 0.5 : 0.5 : 5 : 1 : 2 ms. All gradients were followed by a 500-μs gradient recovery delay. All NOESY1D spectra were acquired with a 500-ms nOe mixing time. All spectra were collected with a spectral width of 8 kHz centered at a 5-ppm proton chemical shift and transformed without any sensitivity or resolution enhancement. The Hadamard editing was done by appropriate addition or subtraction of the FIDs before transformation. During the transformation of each of the HEX-edited NOESY1D spectra (in Figs. 5 and 6), a 10-Hz digital filter was used at the other three frequencies to suppress dispersive artifacts (typically $< 0.5\%$) due to improper cancellation. All spectra (in Figs. 3–6) were plotted with the vertical scaling factor adjusted to the same noise amplitude to allow direct comparison of the signal height. However, the noise insets (in Figs. 3–6) are plotted in absolute intensity scale for direct comparison of the noise level.

CONCLUSION

The DPFGSE-NOE experiment is for all practical purposes superior to the conventional steady-state difference method (1). It provides the sensitivity of the conventional steady-state spectrum but has none of the subtraction artifacts evident in the latter. The HEX-NOESY1D experiment, however, is a cancellation experiment and thus to some extent reduces the advantages of the DPFGSE-NOE experiment over the traditional nOe difference experiment. We find this limitation to be minimal (the

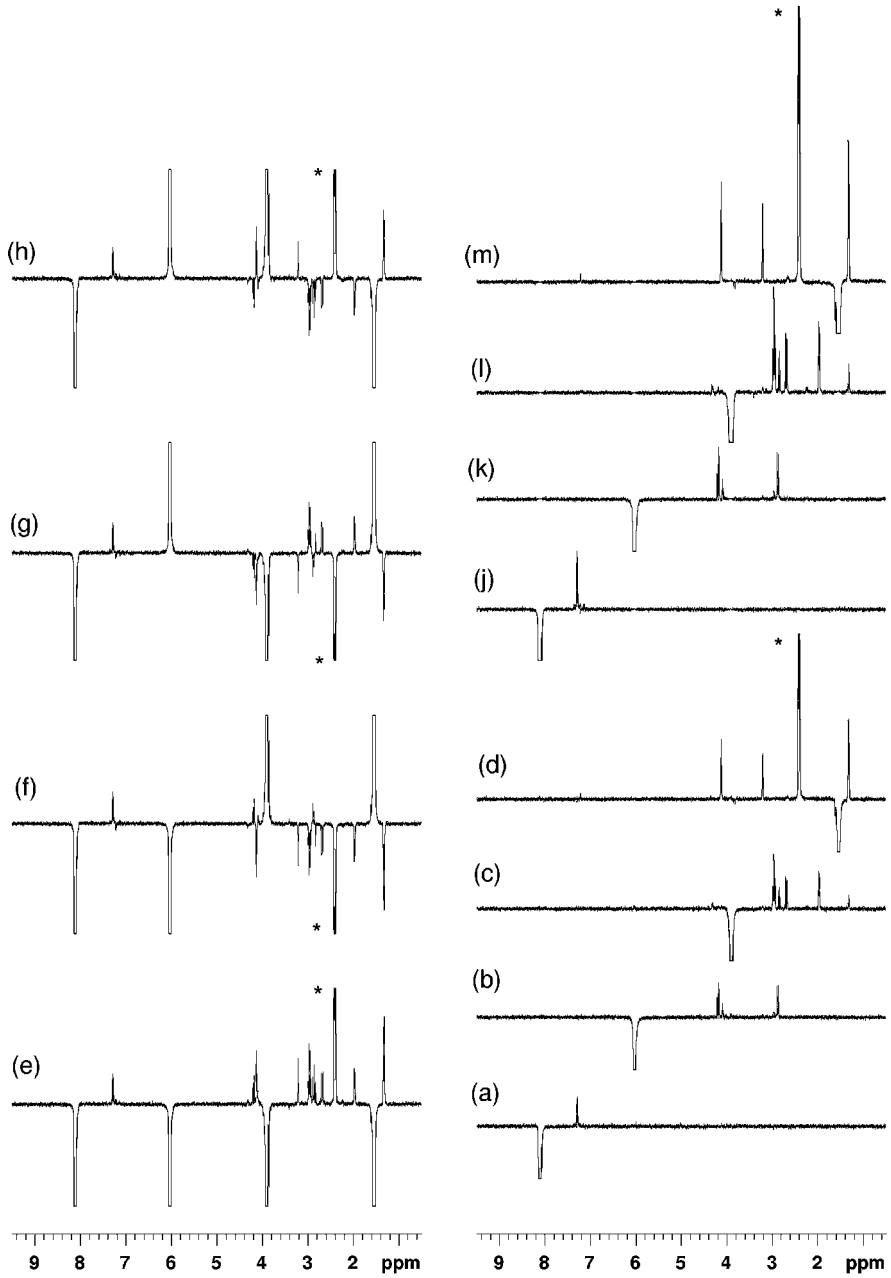

FIG. 5. HEX-NOESY1D spectra of strychnine in CDCl3. (a–d) Single-frequency selected DPFGSE-NOE spectra using the pulse sequence in Fig. 1B with $S_1 = S_2$, (e–h) quadruple-frequency selected HEX-NOESY1D spectra with $S_1 = S_{xxxx}$ and $S_2 = S_{xxxx}$, S_{xxyy}, S_{xyxy}, and S_{xyyx}, and (*j–m*) Hadamard-edited NOESY1D spectra resulting from an appropriate linear combination of the spectra in (e–h). The spectra were obtained using the pulse sequence in Fig. 1B. The band-selective π pulses (S_1 and S_2) are frequency-shifted laminar Q3 pulses. S_{xxxx}, S_{xxyy}, S_{xyxy}, and S_{xyyx} represent that the nominal phase of the quadruple-frequency shifted waveforms are either in-phase (x and x) or quadrature shifted (x and y) with respect to each other. The nonselective π pulses during the mixing time are unshifted hyperbolic secant broadband inversion pulses of 1.5 ms duration. All spectra were acquired with a 500-ms nOe mixing time and 64 scans each. The total acquisition time for all four HEX-NOESY1D spectra (e–h) was 18 min (4.5 min each). The single-frequency selected DPFGSE-NOE spectra (a–d) were collected under conditions identical to those of the HEX-NOESY1D spectra and the total experiment time for all four was 18 min (4.5 min each). The peaks marked with an asterisk ($*$) as well as the "selected" resonances are truncated.

maximum residual cancellation artifact we observed is <0.5%) as any improper cancellation artifact, for all practical purposes, is restricted to the "main" resonances that are canceled during the Hadamard addition/subtraction. The ability to introduce Hadamard encoding in excitation sculpting, as shown in this report, thus provides a way to decrease the total experimental time when selective 1D experiments on more than one resonance is to be performed. We are further exploring ways to exploit

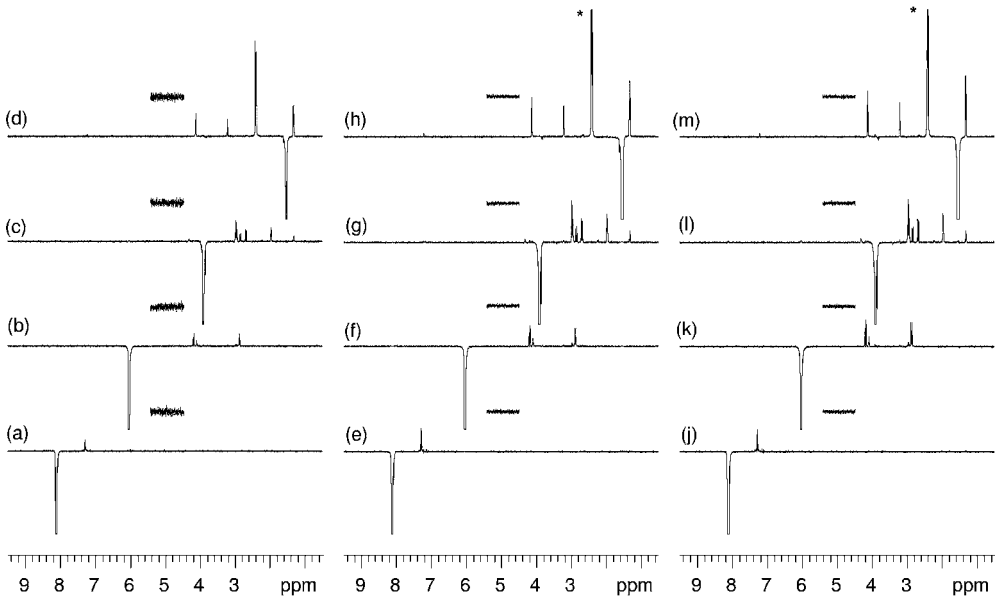

FIG. 6. Comparison of HEX-edited NOESY1D spectra of strychnine in CDCl3 with DPFGSE-NOE spectra collected with one frequency selection at a time. The traces in (a–d) are the same as those shown in Figs. 5a–5d. These were acquired with a 500-ms mixing time and 64 scans each with a total acquisition time of 18 min (4.5 min each). The traces in (e–h) are HEX-edited NOESY1D spectra generated using Hadamard editing of HEX-NOESY1D spectra shown in Figs. 5e–5h. These were also acquired with a 500-ms mixing time and 64 scans each with a total acquisition time of 18 min (4.5 min each). The traces in (j–m) are DPFGSE-NOE spectra collected with one frequency selection at a time. The experimental parameters are identical to those in Figs. 5a–5d, except these were collected over 256 scans, each with a total acquisition time of 72 min (18 min each). The peaks marked with an asterisk (∗) as well as the "selected" resonances are truncated in their height. A 1.0-ppm noise region from each spectrum is further expanded.

the HEX-sculpting technique in two-dimensional experiments to improve resolution/sensitivity and/or reduction in experimental time. These results will be reported elsewhere.

REFERENCES

1. K. Scott, J. Stonehouse, J. Keeler, T. L. Hwang, and A. J. Shaka, *J. Am. Chem. Soc.* **117,** 4199 (1995).
2. S. L. Patt, *J. Magn. Reson.* **96,** 94 (1992).
3. V. V. Krishnamurthy, *J. Magn. Reson. A* **121,** 33 (1996).
4. V. V. Krishnamurthy, *J. Magn. Reson. B* **112,** 75 (1996).
5. V. V. Krishnamurthy, *J. Magn. Reson. B* **113,** 46 (1996).
6. V. V. Krishnamurthy, *Magn. Reson. Chem.* **35,** 9 (1997).
7. Q. N. Van and A. J. Shaka, *J. Magn. Reson.* **132,** 154 (1998), and references therein.
8. C. Gailett, C. Lequart, P. Debeire, and J. M. Nuzillard, *J. Magn. Reson.* **139,** 454 (1999).
9. R. Kaiser, *J. Magn. Reson.* **15,** 44 (1974).
10. R. Freeman and V. Blechta, *Chem. Phys. Lett.* **215,** 341 (1993).
11. V. Blechta, F. del Rio-Portilla, and R. Freeman, *Magn. Reson. Chem.* **32,** 134 (1994).
12. J. Hadamard, *Bull. Sci. Math.* **17,** 240 (1893).
13. T. Nishida, G. Widmalm, and P. Sandor, *Magn. Reson. Chem.* **33,** 596 (1995).
14. T. Nishida, G. Widmalm, and P. Sandor, *Magn. Reson. Chem.* **34,** 377 (1996).
15. For convenience, in this discussion, nominal phase is defined as the ***"end phase"*** of the individual waveforms that are being added to generate the multiple-frequency selected pulse. For refocusing pulses [such as S_1 and S_2, in this case] the relative phase of two waveforms should be ideally defined at the midpoint of the pulse. However, we find that when used in a DPFGSE train shapes with multiple waveforms with their relative phase defined at the beginning, middle or the end of the pulse produces the same result.
16. L. Emsley and G. Bodenhausen, *J. Magn. Reson.* **97,** 135 (1992).
17. E̅. Kupče and R. Freeman, *J. Magn. Reson. A* **105,** 234 (1993).